Stretching Failure Prediction in LS-PrePost® by a SCL Realized Ductile Failure Criterion

Z.Q. Sheng
Body Manufacturing
General Motors Company

Abstract

The LS-PrePost Scripting Command Language (SCL) is a C like computer language that executed inside LS-PrePost. The SCL enables user to process the simulation results and visualize the resultant data back in the LS-PrePost. In this study, the SCL is used to realize a proposed ductile failure criterion (DFC). With the help of the SCL, the stretching failure in the draw simulation results can be predicted. The effectiveness of SCL is demonstrated by a convenient realization of the proposed DFC, which accurately predicts failure in a rectangular cup draw FEM simulation.

Introduction

The LS-PrePost Scripting Command Language (SCL) is a C like computer language that executed inside LS-PrePost. The SCL enables user to process the simulation results and visualize the resultant data back in the LS-PrePost [1]. In previous study, a ductile failure criterion (DFC) for predicting sheet metal forming limit was proposed by the author of this paper. In the proposed DFC, the stretching failure is defined at localized necking or fracture without localized necking, and the critical damage is defined as a function of strain path and initial sheet thickness [2]. The criterion aims to provide a faithful reflection of micromechanical findings on critical damage and to remove post-necking deformation caused uncertainty on forming limit definition. The effectiveness of the proposed criterion has been demonstrated by predicting FLCs for different sheet materials, such as mild steel, advanced high strength steel (AHSS), and aluminum alloys, under linear and quasi-linear strain paths ranging from uniaxial tension (UT) to equal biaxial tension (EBT) [2, 3, 4]. Recently, the model is extended to predict forming limit at low stress triaxiality domain, which is from uniaxial tension (UT) to pure shear (PSH), by introducing a normalized maximum in-plane shear stress factor [5]. Thanks to the function of LS-PrePost SCL, the proposed criterion can work with FEM simulation results, which are calculated by using LSDYNA explicit solver, in an uncoupled manner. In this study, the realization of the DFC by using SCL will be introduced. In the following session, the DFC will be introduced first. Then, the procedure of using SCL to realize the DFC in LS-PrePost will be introduced. Finally, the SCL realized DFC will be used to predict stretching failure in a rectangular cup draw simulation.

Model of the Ductile Failure Criterion

In sheet metal forming, the sheet material primarily experiences tension dominant deformation under strain paths ranging from UT to EBT. At some area, such as the die curve, the sheet material may experience a combination of tension and compression, under which the so-called shear fracture may happen [6]. To model the hybrid effect of tension and shear, a normalized maximum in-plane shear stress component is introduced into the previous proposed DFC and the DFC becomes:

$$f(t_0, \rho) D_{cri}^{UT} = \int_0^{\bar{\varepsilon}^n} (\eta + \langle \psi \rangle \bar{\tau}) d\bar{\varepsilon} \quad (1)$$

where, $\bar{\varepsilon}^n$ is the effective plastic strain at failure, which is defined at LN for stretching mode and shear fracture for shear mode. The effect function $f(t_0, \rho)$ in Eq. (1) reflects the effect of strain path, which is represented by the incremental strain ratio ρ, and initial sheet thickness t_0 on the critical damage. ρ is a ratio of incremental minor strain to major strain ($\rho = \frac{d\varepsilon_2}{d\varepsilon_1}$), which defines the flow direction at the moment of evaluation. Along the strain path of UT, the effect function is chosen at unity for a reference of other strain paths. Using a simple form of McClintock model [2], the absolute damage growth is defined by the integration of η, which is stress triaxiality ratio $\eta = \frac{\sigma_H}{\bar{\sigma}}$ (a ratio of hydrostatic stress σ_H to the effective stress $\bar{\sigma}$). D_{cri}^{UT} is the critical damage under UT and can be expressed by a corresponding limit strain as shown in Eq.(4). To reflect the shear effect at region between UT and PSH, $\langle\psi\rangle\bar{\tau}$ is introduced. $\bar{\tau}$ is a normalized shear stress factor $\bar{\tau} = \frac{\tau}{\bar{\sigma}}$ (a ratio of in-plane maximum shear stress $\tau = (\sigma_1 - \sigma_2)/2$ to the effective stress $\bar{\sigma}$) while ψ is defined as below:

$$\psi = \begin{cases} 0, & \rho^{UT} < \rho \\ \frac{\rho^{UT} - \rho}{1 + \rho^{UT}}, & -1 \le \rho \le \rho^{UT} \end{cases} \quad (2)$$

to reflect the shear effect starting after strain ratio is lower than ρ^{UT}, which is the strain ratio at UT. From strain path UT to PSH, the ψ represents the shear stress effect increases from zero at UT as a linear function of ρ and becomes unity at PSH, which represents the increase of compression and its dominancy at pure shear.

Realization of uncoupled damage calculation with FEM simulation by SCL

Working with a FEM simulation in an uncoupled manner, the relative damage growth of any element on a deformed sheet material can be calculated as:

$$D = \frac{1}{\langle f(t_0,\rho)\rangle D_{cri}^{UT}} \int_0^{\bar{\varepsilon}^n} (\eta + \langle\psi\rangle\bar{\tau}) d\bar{\varepsilon} \quad (3)$$

where, $f(t_0, \rho)$ can be summarized as:

$$f(t_0,\rho) = \begin{cases} (1+\rho+2\rho^2)\left(1 + 2(\rho+0.5)\left(1 - \frac{f(t_0,-1)}{2}\right)\right), & -1.0 \le \rho \le -0.5 \\ (1+\rho)(f(t_0,0) + 2(f(t_0,0)-2)\rho, & -0.5 < \rho \le 0 \\ (1+\rho)\left(f(t_0,0) + (-0.414\rho^2 + 1.414\rho)\left(0.5f(t_0,1) - f(t_0,0)\right)\right), & 0 < \rho \le 1 \end{cases}, \quad (4)$$

A detail derivation of Eq.(4) and effect functions $f(t_0,-1),\ f(t_0,0), and\ f(t_0,1)$ at strain paths of PSH, plane strain (PS) and EBT can be found in [2, 5]. At each time step of calculation, a linear strain path is assumed. A failure is reported when the relative damage value *D* reaches unity. It should be noted that the parameter t_0 is a constant value for each target sheet material and thus does not change during forming simulation. When the deformation is in thickening mode (calculated η<0), the η and $\bar{\tau}$ are set to zero to reflect that the wrinkling risk becomes dominant while the stretching failure is not regarded as a primary consideration. The criterion is realized by using SCL in a procedure shown in Figure 1. To predict stretching failure, in the LS-PrePost environment, the simulation results, which are calculated by LS-DYNA® solver, are loaded first. Then, SCL file is loaded through an interface shown in Figure 2. The DFC that is encoded by SCL file is then interpreted by the LS-PrePost in a procedure as shown in Figure 1. At each state, the stress and strain information of each element is read and relative damage is calculated. The calculation continues until the end of simulation. Then the resultant relative damage is fringed on the LS-PrePost.

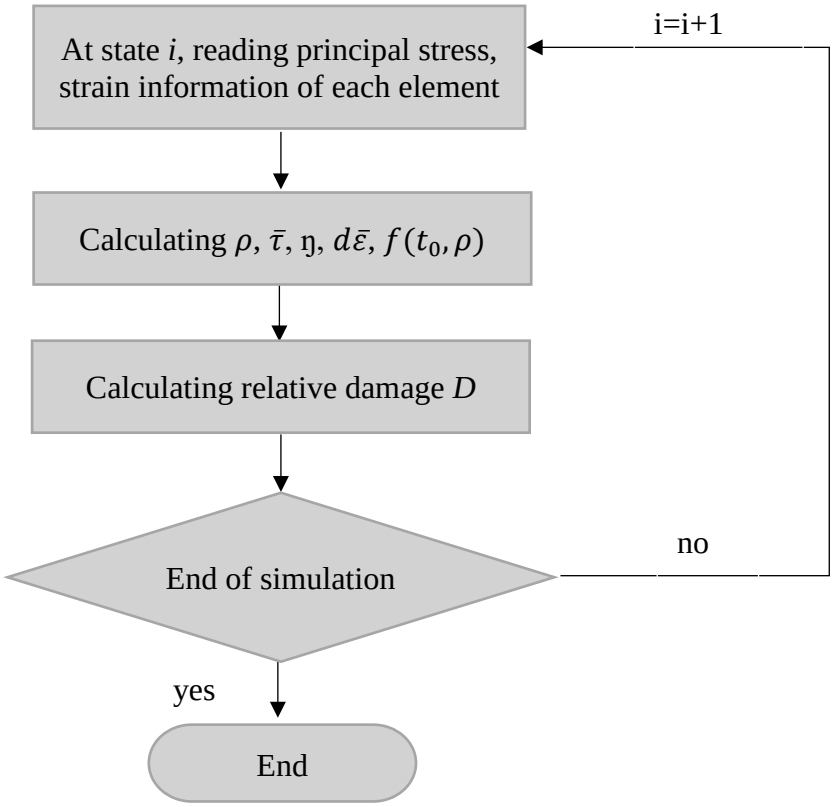

Figure 1 Flow chart of realization the DFC by using SCL

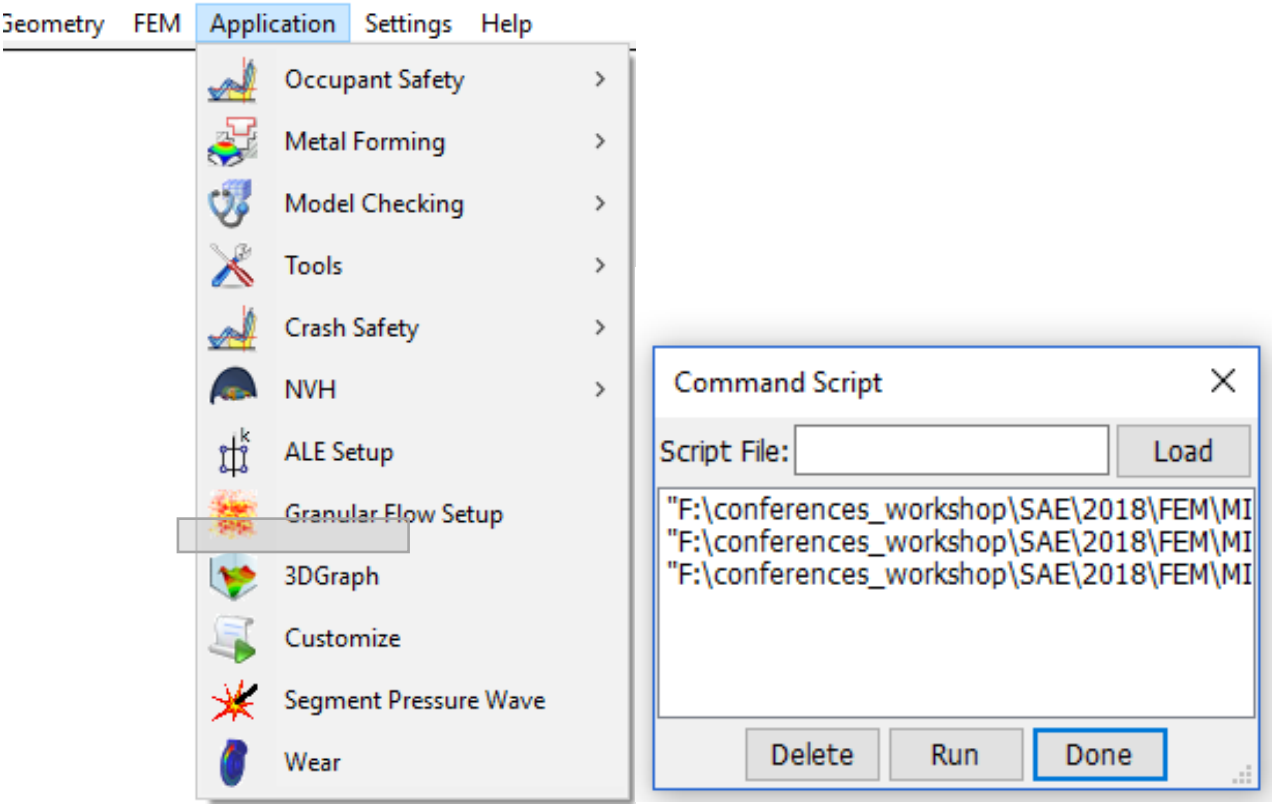

Figure 2 Interface of loading SCL file in LS-PrePost 4.3

Predicting failure in TRIP 690 steel cup draw

The effectiveness of the SCL realized DFC is demonstrated on predicting stretching failure in a rectangular cup draw simulation on 1.6 mm thick TRIP 690 sheet material. Table 1 gives the material properties of the sheet material. The DFC is calibrated by using the forming limit data given in [6]. Based on the low boundary measurement at LN from dome test and shear fracture in [6], the major limit strains at strain paths of PSH, UT, PS, and EBT are measured at 0.58, 0.42, 0.25, and 0.35. Correspondingly, the effect function at strain path of PS, EBT, PSH are calculated at 1.095 3.333, and 2.762, respectively [6].

A detail introduction of the cup draw test can be found in [6]. Figure 3 gives the setup of sheet blank and FEM model of the rectangular cup draw in LS-PrePost-4.3. The punch, die and binder are treated as rigid bodies and modeled by shell elements with an average mesh size 2 mm and thus have more than six elements distributed over radius areas. Sheet blank is modelled by 22680 quad shell elements with a uniform mesh size of 1 mm x 1 mm. Material model 37 (MAT 37) in LS-DYNA, which uses Hill-48 for yielding surface, is selected to describe the elastic-viscoplastic behavior of the sheet material. A mass scaling (6400%) is selected to reduce the computation cost while the kinematic energy is kept below 1% of internal energy.

Table 1. Mechanical properties of 1.6 mm thick TRIP 690 [6]

UTS (MPa)	K (MPa)	n	r bar
690.0	1276.0	0.27	1.0

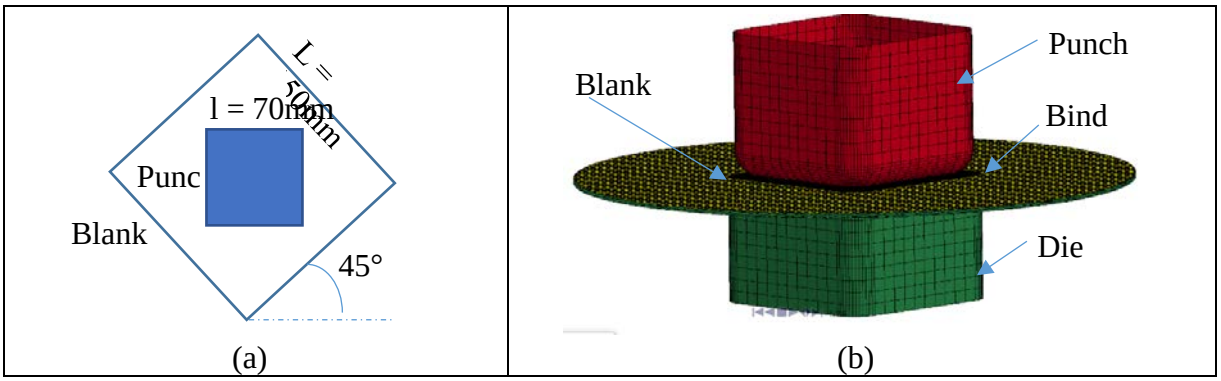

Figure 3. Model of rectangular cup draw: a. setup of sheet blank orientation; b. FEM model

Based on [6], the binder clamping and punch drawing are modeled in two consecutive steps. After binder clamping, a binder force of 30 kN is applied. Then, punch travels at a constant speed of 35 mm/s to reflect the boundary condition in the test. During punch travel, die is fixed while blank holder allows free movements in the punch travel direction. A constant Coulomb friction coefficient of 0.17 is chosen to model the interfacial friction between tooling components and sheet blank.

Figure 4(a) shows the calculated relative damage distribution at the top surface (towards die cavity) of the numerically formed cup. At the draw depth of 22 mm, the calculated relative damage of the top surface reaches unity at corner of punch radius. The predicted failure matches well with the observation on the physical cup [6]. Figure 4 (b) plots the relative damage growth on the critical element, at which the localized necking initiates. Figure 4 (c) gives the strain path of the critical element, which exhibits a nonlinear trajectory. However, at same draw depth, shear fracture risk is overestimated at the bottom surface at die curve area as shown in Figure 3 (d). Similar overestimation was reported in [6] as well. Figure 3 (e) shows the nonlinear strain path of the critical element on the bottom surface, which exhibits a strain path varying from PSH to UT. The observed

overestimation of damage on the bottom surface could be due to strain path effect in the region between PSH and UT, which may not as strong as that in the region between UT and EBT. To prove the hypothesis, when the deformation is in the region between PSH and UT, the strain ratio ρ, is calculated as ratio between accumulated minor strain and major strain ($\rho = \frac{\varepsilon_2}{\varepsilon_1}$) at the moment of evaluation to reduce the variation of strain ratio change at each time step. Figure 3(f) shows that the overestimated risk of failure on the bottom surface is removed. To further study the strain ratio represented strain path effect, average strain ratio for each element is calculated as below:

$$\bar{\rho} = \frac{\int_0^{\bar{\varepsilon}} \rho d\bar{\varepsilon}}{\bar{\varepsilon}} \quad (5)$$

When the ρ in Eq.(4) is replaced by $\bar{\rho}$, as shown in Figure 4(g), the stretch failure initiation is detected at same draw depth of baseline prediction as shown in Figure 4 (a). However, the failure initiates at a location slightly lower than that in the baseline result. On the other hand, as shown in Figure 4 (h), at same draw depth, the relative damage at bottom surface does not show a risk of shear fracture as that shown in the Figure 4(d).

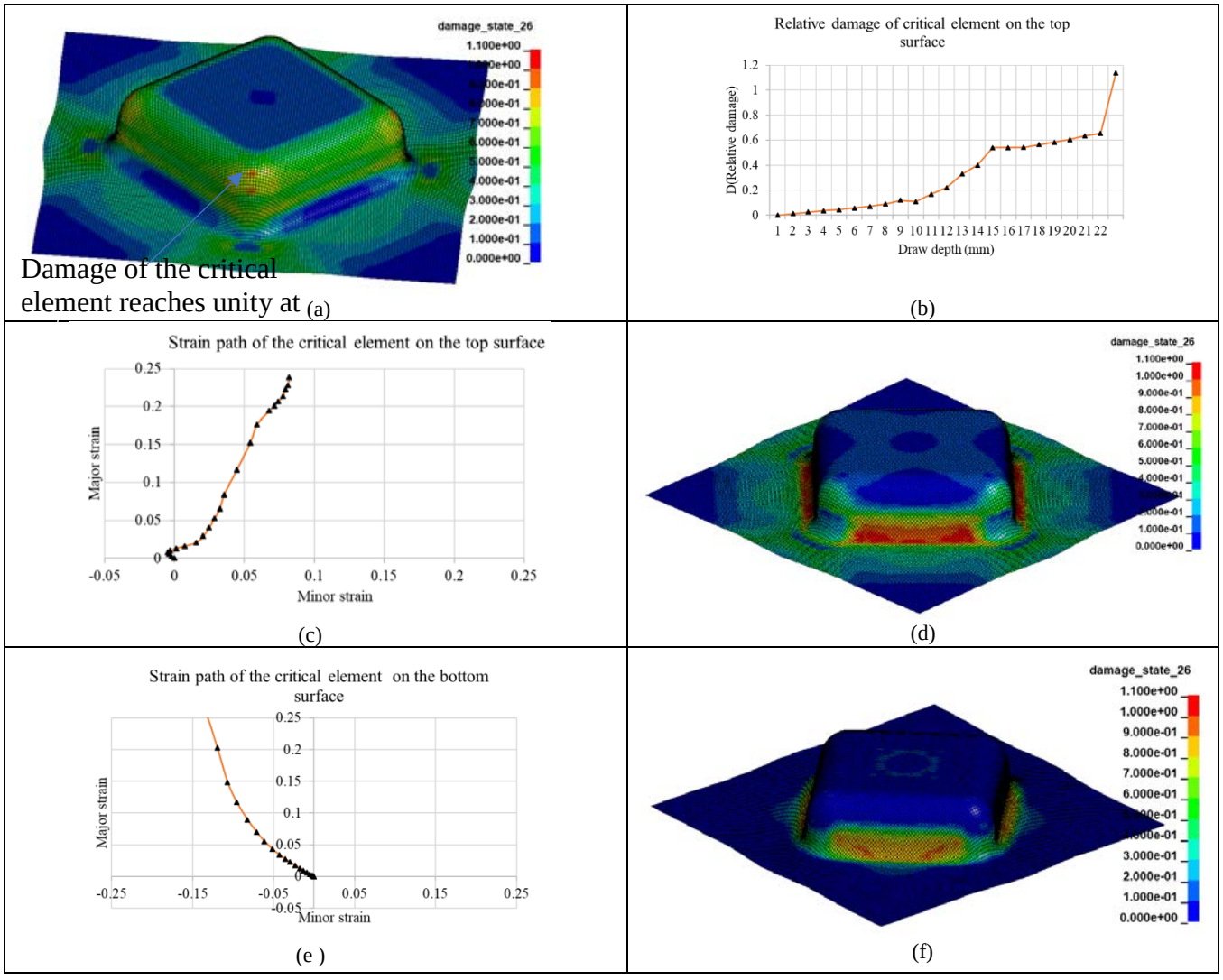

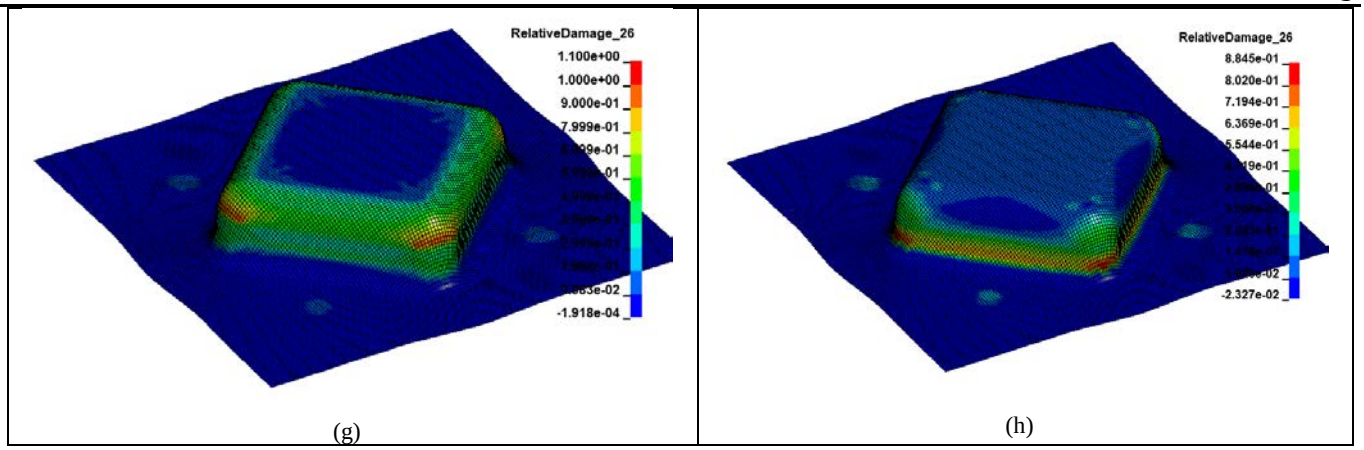

(g) (h)

Figure 4 Results of cup draw: (a) damage on the top surface of numerically formed cup, (b) damage growth of the critical element on the top surface, (c) strain path of the critical element on the top surface, (d) damage on the bottom surface of numerically formed cup with overestimated risk, (e) strain path of the critical element on the bottom surface, (f) damage on the bottom surface of numerically formed cup assumed linear strain path at region between PSH and UT, (g)damage on the top surface when average strain ratio is used (h) damage on the bottom surface when average strain ratio is used

Conclusion and discussion

In this study, the realization of a Ductile Failure Criterion by using LS-PrePost SCL for predicting stretching failure in sheet forming simulation is introduced. The effectiveness of the SCL on realizing proposed ductile failure criterion is demonstrated by accurately predicting failure in a rectangular cup draw from TRIP690 sheet material. With the help of SCL, different strategies, for instance, different strain path representations, can be realized and evaluated conveniently.

Acknowledgement

Appreciation goes to Dr.Yuzhong Xiao at LSTC for his quick and effective technical support. The author also would like to thank GM management for the approval of publishing this work.

References

1. Ho, P., LS-PrePost Scripting Command Language and Data Center, Rev.1, July 29, 2015
2. Sheng, Z. Q., & Mallick, P. K. 2017. A ductile failure criterion for predicting sheet metal forming limit. *International Journal of Mechanical Sciences*, *128*, pp. 345-360.
3. Sheng, Z. Q., & Mallick, P. K. 2017. Predicting Sheet Forming Limit of Aluminum Alloys for Cold and Warm Forming by Developing a Ductile Failure Criterion. ASME *Journal of Manufacturing Science and Engineering*, *139*(11), 111018.
4. Sheng, ZiQiang, and Pankaj Mallick. *Predicting Forming Limit Curve Using a New Ductile Failure Criterion*. No. 2017-01-0312. SAE Technical Paper, 2017.
5. Sheng, ZiQiang, and Pankaj Mallick, Modeling Forming Limit in Low Stress Triaxiality and Predicting Stretching Failure in Draw Simulation by an Improved Ductile Failure Criterion, No. 2018-01-0181. SAE Technical Paper, 2018
6. Li, Y., Luo, M., Gerlach, J., & Wierzbicki, T. 2010. Prediction of shear-induced fracture in sheet metal forming. Journal of Materials Processing Technology, 210(14), 1858-1869.